Faraday Discussions

RSC Publishing

Cite this: *Faraday Discuss.*, 2013, **165**, 369

PAPER

View Article Online
View Journal | View Issue

The effects of aircraft on climate and pollution. Part II: 20-year impacts of exhaust from all commercial aircraft worldwide treated individually at the subgrid scale

M. Z. Jacobson,*[a] J. T. Wilkerson,[a] A. D. Naiman[b] and S. K. Lele[c]

Received 8th March 2013, Accepted 16th April 2013
DOI: 10.1039/c3fd00034f

This study examines the 20-year impacts of emissions from all commercial aircraft flights worldwide on climate, cloudiness, and atmospheric composition. Aircraft emissions from each individual flight worldwide were modeled to evolve from the subgrid to grid scale with the global model described and evaluated in Part I of this study. Simulations with and without aircraft emissions were run for 20 years. Aircraft emissions were found to be responsible for ~6% of Arctic surface global warming to date, ~1.3% of total surface global warming, and ~4% of global upper tropospheric warming. Arctic warming due to aircraft slightly decreased Arctic sea ice area. Longer simulations should result in more warming due to the further increase in CO_2. Aircraft increased atmospheric stability below cruise altitude and decreased it above cruise altitude. The increase in stability decreased cumulus convection in favor of increased stratiform cloudiness. Aircraft increased total cloud fraction on average. Aircraft increased surface and upper tropospheric ozone by ~0.4% and ~2.5%, respectively and surface and upper-tropospheric peroxyacetyl nitrate (PAN) by ~0.1% and ~5%, respectively. Aircraft emissions increased tropospheric OH, decreasing column CO and CH_4 by ~1.7% and ~0.9%, respectively. Aircraft emissions increased human mortality worldwide by ~620 (−240 to 4770) deaths per year, with half due to ozone and the rest to particulate matter less than 2.5 micrometers in diameter ($PM_{2.5}$).

1 Introduction

This is a study to quantify the effects of all major components of aircraft exhaust and their resulting contrails, on global and regional climate, cloudiness, and atmospheric composition. The study also aims to examine the contribution of aircraft to Arctic warming. Previous studies of the effects of aircraft exhaust and

[a]*Dept. of Civil and Environmental Engineering, Stanford University, Stanford, CA, USA. E-mail: Jacobson@stanford.edu*

[b]*Exponent Engineering and Scientific Consulting, CA, USA*

[c]*Dept. of Aeronautics and Astronautics, Stanford University, Stanford, CA, USA*

the resulting contrails and gases on climate have been limited primarily to the global-scale radiative forcing due to the exhaust.[1–10] However, direct radiative forcing, which most studies have used to estimate climate effects, is not necessarily proportional to the climate response of aerosols, which is why recent studies have switched to using adjusted forcings and other metrics.[11] Because adjusted forcing itself is an approximate parameter since it requires sea-surface temperature to be held constant, and because it does provide information about air quality, simulating the full climate and air quality response of aircraft without approximation may be the cleanest method of estimating the climate and health effects of aircraft. This type of calculation is performed here.

Previously, Ponater *et al.*[12] and Rind *et al.*[13] examined the global climate response of aircraft water vapor or aircraft-enhanced cirrus. Jacobson *et al.*[14] examined the climate response of rerouting cross-polar flights around the Arctic Circle while treating each flight independently at the subgrid scale. Fromming *et al.*[15] examined the surface temperature response to changing the altitude of flight emissions. Previous studies have not examined the global climate response of major emissions from all commercial aircraft worldwide, particularly when the emissions from each aircraft are tracked individually.

This study uses a global model modified to treat the evolution of individual subgrid aircraft exhaust plumes to simulate the climate and pollution effects of contemporary emissions from all commercial flights worldwide. Short-term (20-year) effects are examined since this is the time scale of relevance to the Arctic sea ice, which is disappearing rapidly, and due to the significant computer time required to run the simulations here.

2 Model description

The model used for this study, GATOR-GCMOM, is described and evaluated with respect to aircraft-relevant parameters in Part I of this study, Jacobson *et al.*,[16] and in Whitt *et al.*[17] and with respect to climate response in Jacobson *et al.*[18] Briefly, it is a one-way nested global-through-local Gas, Aerosol, Transport, Radiation, General Circulation, Mesoscale, and Ocean Model that simulates climate, weather, and air pollution. It treats emissions; gas photochemistry; size- and composition-resolved aerosol and hydrometeor microphysics and chemistry; size- and composition-resolved aerosol-hydrometeor interactions; subgrid cumulus cloud thermodynamics; grid-scale stratiform thermodynamics; spectral radiative transfer for heating rates and photolysis; dynamical meteorology; 2-D ocean dynamics; 3-D ocean diffusion; 3-D ocean chemistry; ocean-atmosphere exchange; and ice, snow, land surface processes, and subgrid contrail formation and aerosol evolution from each individual flight worldwide.

With respect to aircraft, the model accounts for the microphysical evolution of contrails from all commercial aircraft worldwide at the subgrid scale (at their actual size).[16] Briefly, subgrid processes treated include (1) spreading and shearing of individual aircraft exhaust plumes,[19] (2) calculating a unique supersaturation for each plume based on water vapor and aerosol particles emitted during each flight added to existing water vapor and particles, (3) calculating time-dependent, discrete size-resolved ice deposition and condensation followed by freezing onto size-resolved aerosols, (4) calculating size-resolved coagulation to create and grow linear contrails at the subgrid scale, (5) solving for the discrete

size-resolved evolution of grid-scale cirrus and other clouds from the remnants of subgrid linear contrails, and (6) determining radiative effects of subgrid linear contrails as a function of ice crystal size and composition and contrail plume shape and accounting for random overlap of contrails and clouds.

At the grid scale, three discrete (multiple size bin) aerosol size distributions and three discrete hydrometeor distributions, each with multiple components per bin, were treated.[14] The three aerosol distributions were an emitted fossil-fuel soot (EFFS) distribution, an emitted combined biofuel-soot and biomass-burning-soot (BFBB) distribution, and an ultimate internally-mixed (UIM) distribution. Each size distribution contained 14 size bins (2 nm–50 μm diameter). The three hydrometeor distributions included liquid, ice, and graupel, each with 30 size bins (0.5 μm to 8 mm in diameter). Each size bin of the EFFS distribution contained black carbon (BC), weakly-to-moderately-absorbing primary organic matter (POM), secondary organic matter (SOM), hydrated liquid water, H_2SO_4(aq), HSO_4^-, SO_4^{2-}, NO_3^-, Cl^-, H^+, NH_4^+, NH_4NO_3(s), and $(NH_4)_2SO_4$(s). Each size bin of the BFBB distribution contained these same components plus tar balls, Na^+, K^+, Ca^{2+}, and Mg^{2+}. Each size bin of the UIM distribution contained the same components as the EFFS and BFBB distributions plus soil dust, pollen, spores, and bacteria. Each size bin of each hydrometeor distribution contained the same components as in all three aerosol distributions plus condensed liquid water or deposited ice. Gases, such as HNO_3, HCl, NH_3, H_2SO_4, and organics could condense onto or dissolve into grid-scale EFFS, BFBB, and UIM aerosol particles and dissolve within liquid hydrometeor particles or chemically react on ice and graupel hydrometeor particle surfaces.

Discrete size-resolved EFFS, BFBB, and UIM aerosol particles and liquid, ice, and graupel hydrometeor particles and their components could coagulate among each other as a function of size. Thus, grid-scale aerosol particles and their components were tracked within hydrometeor particles through cloud formation and precipitation.

BC, brown carbon (BrC), and soil dust absorption in clouds was treated with the dynamic effective medium approximation (DEMA), which accounted for aerosol particles distributed randomly throughout each hydrometeor particle in the model.[14] Inorganic gases, such as HNO_3, HCl, NH_3, and H_2SO_4, and organic gases could condense onto or dissolve into grid-scale EFFS, BFBB, and UIM aerosol particles. Liquid water could also hydrate to soluble species and ions could crystallize to solid within such particles. EFFS, BFBB, and UIM aerosol particles served as nuclei for new hydrometeor particles. In sum, the model treated indirect, semi-direct, and cloud absorption effects of aerosols on contrails and all other cloud types as a function of size, composition, and spectral wavelength.[14]

Flight-by-flight aircraft emissions used for this study were for 2006.[20] Size-resolved particle components from aircraft (BC, POM, S(VI) = H_2SO_4(aq) + HSO_4^- + SO_4^{2-}) and water vapor were emitted into subgrid plumes. Size- and composition-resolved contrail particles formed and grew onto the subgrid size-resolved aerosol particles by nucleation, water deposition, and coagulation. CO, CO_2, SO_2, NO_x, and speciated total hydrocarbons (THCs) from aircraft were emitted directly to the grid scale. When contrails in subgrid plumes dissipated due to plume expansion and dilution and ice sublimation, then water vapor and size- and composition-resolved aerosol cores containing BC, POM, and S(VI) from

them were released from each plume to the grid scale in the EFFS aerosol distribution, where the particles affected clouds and radiation. The grid-scale EFFS distribution also contained emissions from other fossil-fuel sources.

3 Simulations

A pair of 20-year global (non-nested) simulations was first run. One simulation included all gas and particle aircraft emissions (baseline simulation), and the other (sensitivity simulation) did not. Six additional simulations, each with a random initial perturbation, were run to test the statistical significance of results through a two-sample t-test.

The horizontal grid scale resolution was 4°-SN × 5°-WE. The model included 68 vertical sigma-pressure layers from the ground to 0.219 hPa (≈60 km), with 15 layers from 0–1 km and 500 m resolution from 1–21 km. The center of the lowest model layer was 15 m above ground. Since all flights in the Enhanced Traffic Management System (ETMS) occur at 41 000 ft (12.5 km) or below, the 500 m resolution up to 21 km was sufficient.

All simulations were initialized with 1° × 1° reanalysis fields for 12 GMT of the start date of simulation.[21] Aircraft emissions for 2006 were repeated each year. Following initialization, the model was entirely prognostic (no data assimilation or nudging).

Although complete temperature responses, particularly of CO_2, require much more than 20 years, the purpose of this study is to examine the estimated impact of aircraft over the short term since that is relevant to the loss of Arctic sea ice, which may disappear over this time frame.

4 Results

Fig. 1–4 provide simulation-averaged difference (with minus without aircraft) information of the modeled aircraft effects on climate and atmospheric composition. A simulation-averaged value is one in which values of the parameter are summed over all time steps and the sum is divided by the number of time steps. In all cases, results are for grid-scale parameters or, in the case of contrail water, combined over all subgrid contrails.

4.1 Effects on atmospheric gas and aerosol composition

Aircraft emissions (at the subgrid scale) peak vertically between 10–12 km (265-194 hPa) above sea level.[20] This was the height range in which changes in modeled aerosol particle number, SO_2, NO_2, and contrail water peaked (Fig. 1a–d). Horizontally, such peaks occurred from 30–90 N.

Above 9 km (300 hPa), aircraft nearly doubled the concentration of BC in the EFFS aerosol size distribution (Fig. 1e) and increased BC by about 7% in the UIM distribution (Fig. 1f). BC emissions from aircraft represent a small percent (0.21%) of globally-emitted BC from all submicron fossil-fuel BC sources and even less (0.09%) from submicron fossil-fuel plus biofuel plus biomass-burning sources. Thus aircraft are a proportionately larger relative contributor to upper tropospheric and stratospheric BC than are other sources of BC. The result makes sense because most surface-emitted BC is removed with a lifetime of a few days[14] and the upper-troposphere/lower stratosphere (UTLS) is stable,[17] so surface BC

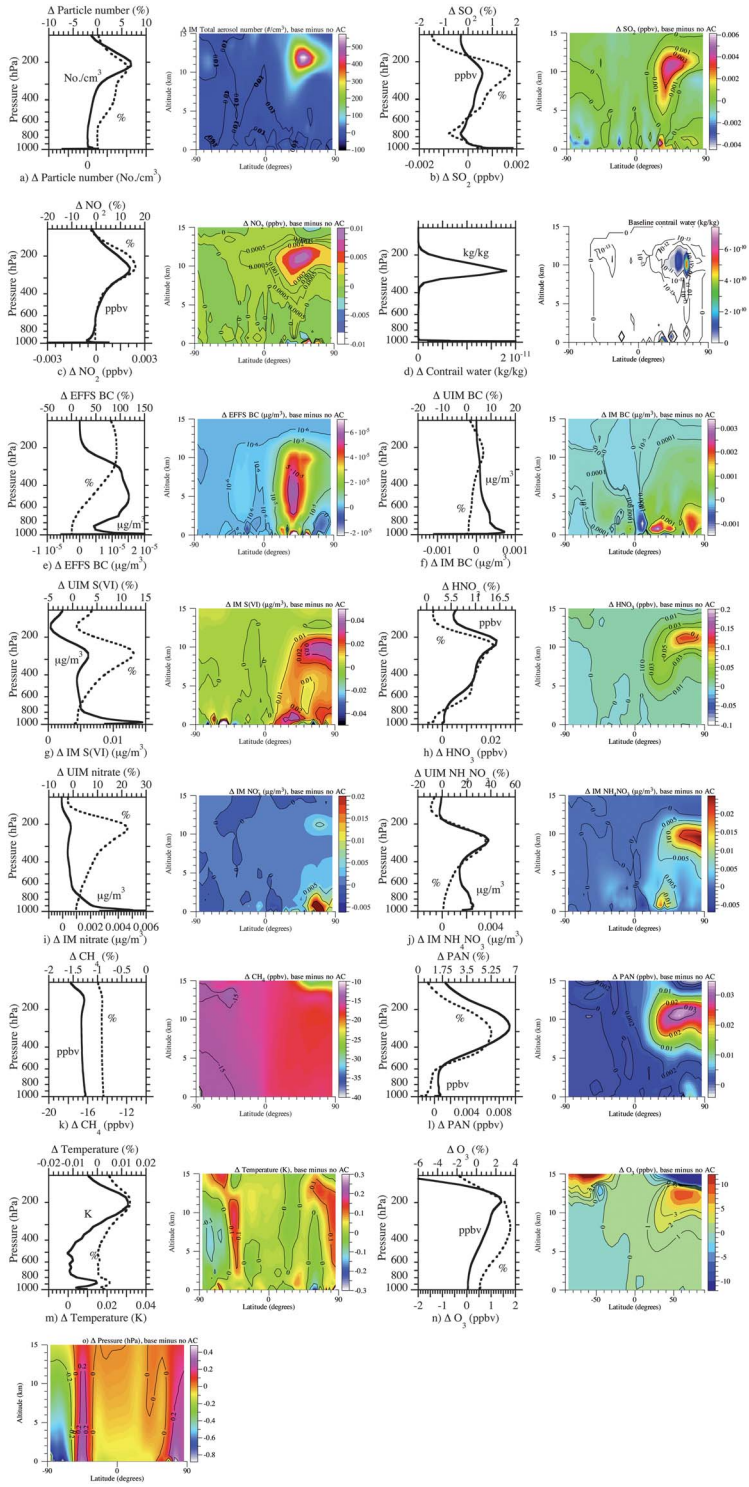

has difficulty rising to that height, whereas aircraft BC is emitted directly to the UTLS.

BC, POM, and S(VI) emitted into each aircraft exhaust plume either stayed as aerosol or served as nuclei for contrail formation. When the exhaust plume expanded sufficiently so that the contrail disappeared, the aerosol material was added to the grid-scale EFFS aerosol size distribution. Such aged and partly internally-mixed particles eventually coagulated with aerosol particles from other sources in the EFFS, BFBB, or UIM aerosol distributions to become UIM particles or larger EFFS particles, or they coagulated with hydrometeor particles or served as cloud deposition or condensation nuclei. EFFS coagulation with other aerosol particles resulted in an increase in internally-mixed BC and S(VI), particularly at cruise altitude from 30–90 N by about 7% and 12%, respectively (Fig. 1f and 1g). The increase in NO_x due to aircraft increased nitric acid available at cruise altitude (Fig. 1h). Some nitrate ion reacted with the ammonium ion to form ammonium nitrate (Fig. 1j) at cruise altitude.

Aircraft increased upper-tropospheric NO_x, not only by emitting anthropogenic NO_x but also by increasing lightning production of NO_x (Fig. 2a). Aircraft increased the number of liquid and ice cloud nuclei (*e.g.*, Fig. 1a), increasing the number of ice cloud particles in convective clouds, increasing the number of size-resolved hydrometeor particle collisions and charge-separating ice–ice, ice–liquid, and liquid–liquid bounceoffs, increasing the buildup of charges and probability of lightning. Jacobson and Streets[22] describe the equations describing modeled lightning.

The increases in aircraft-emitted H_2O (which reacts with $O(^1D)$ to form 2OH), NO (which reacts with HO_2 to form OH), HCHO, and CH_3CHO (which photolyze to OH) all increased tropospheric OH (Fig. 2b). Enhanced OH-oxidized CO (Fig. 2c) and CH_4 (Fig. 1k) to CO_2, decreasing column CO and CH_4 by $\sim$1.7% and $\sim$0.9%, respectively. Thus, despite the fact that aircraft increased CO emissions, CO mixing ratios decreased due to aircraft because the higher OH resulting from aircraft converted both emitted and background CO (and CH_4) to CO_2, reducing both CO and CH_4 mixing ratios. Most CO and CH_4 decreases were in the Northern Hemisphere in locations where most OH increases occurred. The reduction in CH_4 due to aircraft exhaust is well known.[10]

Higher NO_x (Fig. 1c) coupled with small changes in acetaldeheyde increased surface and upper-tropospheric PAN by 0.1% and 5%, respectively (Fig. 2t) and column PAN by 2.6%. Increases in tropospheric PAN peaked near where aircraft contrails peaked (Fig. 1h).

Higher NO_x, organics, and temperatures (Fig. 1m) due to aircraft caused O_3 to increase by $\sim$0.4% at the surface and $\sim$2.5% ($\sim$2.5 ppbv) at cruise-altitude (Fig. 1n). Köhler *et al.*[23] and Lee *et al.*[10] similarly concluded that aircraft increase cruise-altitude O_3. Immediately above cruise altitude, ozone decreased in the presence of aircraft because aircraft increased mid-to-lower stratospheric stability

Fig. 1 Globally- and simulation-averaged vertical profile differences and zonally- and simulation-averaged differences in several modeled parameters between the simulations with *versus* without aircraft. All parameters shown are grid-scale parameters, except that contrail water is summed over all subgrid contrails. For reference, altitudes are roughly correlated with the following pressures (5 km: 540.5 hPa; 10 km: 265 hPa; 15 km: 121.1 hPa).

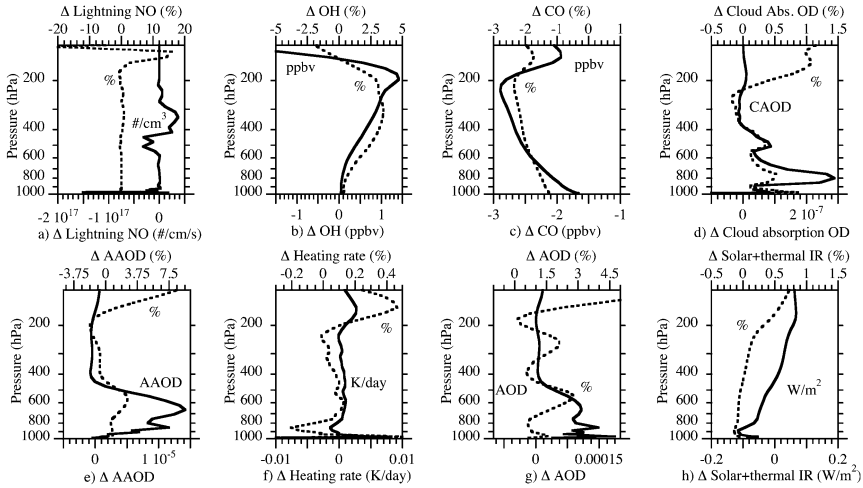

Fig. 2 Same as Fig. 1, but for globally- and simulation-averaged vertical profile differences for some additional parameters.

(not seen in Fig. 1m), reducing the downward transport of ozone from the ozone layer to the UTLS region.

Aircraft exhaust increased surface O_3 by 0.05 ppbv worldwide on average and by a peak of > 1 ppbv (Fig. 3a) by increasing emissions of ozone precursors. The estimated premature mortality rates due to enhanced 8-hr averaged ozone were calculated as ~310 (160 to 470) per year. Dry $PM_{2.5}$ and total $PM_{2.5}$ increased, in the global average, by 0.083 μg m^{-3} and 0.54 μg m^{-3} (Fig. 3d, e). Estimated premature mortalities, based on dry $PM_{2.5}$ are ~310 (−400 to 4300) per year. These mortality numbers were obtained during the model simulation by combining current mixing ratios or concentrations predicted by the model each time step in each model grid cell with population data for each cell and relative risks, all in a health effects equation, as described previously.[24]

4.2 Effects on contrails, clouds, and precipitation

Aircraft exhaust affected contrail, cumuliform, and stratiform cloud properties through both microphysical (indirect) and radiative effects of aerosols on clouds and through feedbacks of exhaust to temperatures, relative humidities, and winds. The Northern Hemisphere (NH) contrail cloud fraction change (+0.0030) due to aircraft exceeded that in the Southern Hemisphere (SH) (+0.000062) by a factor of 48 (Fig. 3f). The NH total cloud fraction increase (+0.12%) exceeded that in the SH (+0.018%) by a factor of 7 (Fig. 3g). Aircraft increased grid-scale in-cloud ice number concentration (Fig. 3h) due to the increased number of aerosol particles from aircraft that can serve as ice nuclei.

Cloud absorption optical depth (CAOD) was calculated by tracking BC, BrC, and soildust in each size bin of liquid, ice, and graupel hydrometeor particles and applying the iterative dynamic effective medium approximation (DEMA), assuming that nucleated and scavenged aerosol particles were randomly distributed in the hydrometeor particles.[14] Aircraft increase CAOD by up to 1% (Fig. 2d) and AAOD by up to 7.5% (Fig. 2e) in the global average above 11.8 km

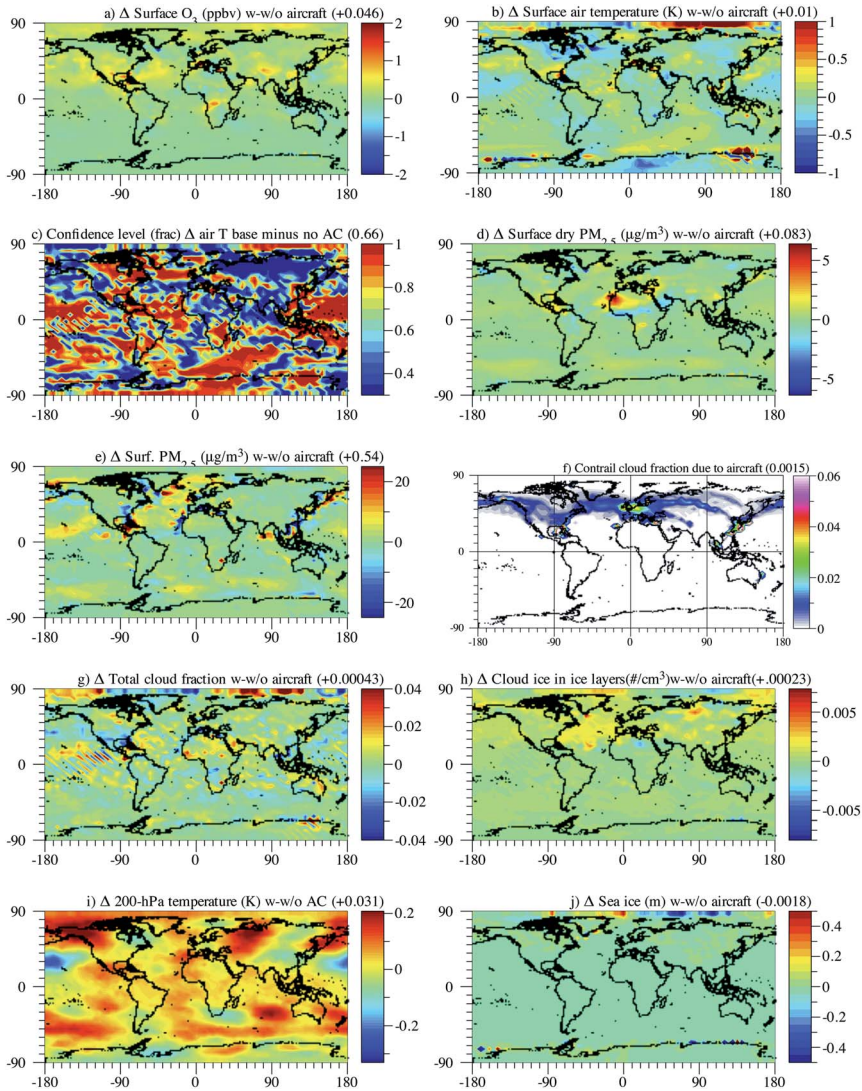

Fig. 3 Simulation-averaged spatial differences in several modeled parameters (surface or column-integrated) between when aircraft emissions of gases and particles were and were not included. Also shown, for one figure, is a corresponding plot of the confidence level of the results from a 2-sided t-test relative to six random perturbation simulations during the simulations.

(200 hPa). The enhanced absorption increased the heating rate in this altitude range by up to 0.5% (Fig. 2f) and the temperature by up to 0.015% in the global average (Fig. 1m). EFFS BC increased by up to 100% (Fig. 1e) and UIM BC, by up to 7% (Fig. 1f) in this region. The vertical spread of BC above cruise was helped by enhanced instability at and just above cruise altitude (Fig. 1m).

Increases in CAOD in a given location were due to both an increase in aircraft BC within clouds in that location and a local reduction in precipitation from clouds. A reduction in precipitation increases total cloud material, including BC, thus it increases CAOD. Aircraft decreased precipitation by 0.16% in the global

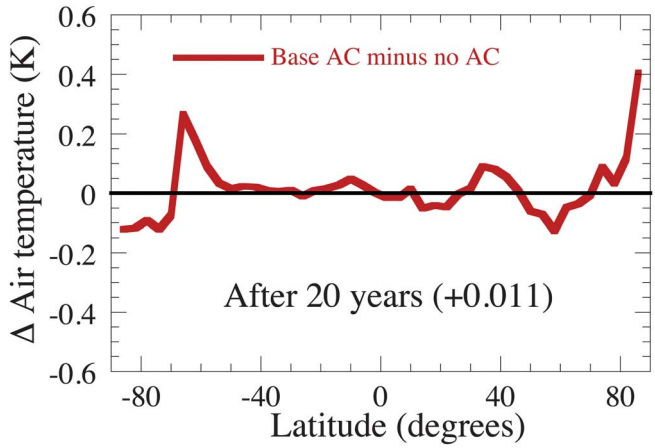

Fig. 4 Zonally- and simulation-averaged surface air-temperature difference between the baseline case with aircraft emissions and the simulation with no aircraft emissions.

average, 0.36% in the Northern Hemisphere, and 0.0038% in the Southern Hemisphere during the simulations.

Aircraft increased stratus (including cirrus-type) cloud fraction by 0.2%, decreased cumulus cloud fraction by 0.19%, and total cloud fraction by +0.065% in the global average. These numbers were +0.34%, −0.47%, and +0.12%, respectively, in the Northern Hemisphere. Total cloud fraction increases occurred significantly in the Arctic regions (Fig. 2f). The reduction in cumulus cloud fraction occurred because aircraft stabilized the troposphere below cruise altitude by increasing cruise-altitude temperatures more than surface temperatures (Fig. 1m). The reduction in cumulus also reduced precipitation, as previously discussed, and enhanced stratus since the water vapor in the air still needed to condense. Increases in cloud condensation nuclei (CCN) and ice deposition nuclei (IDN) due to an increase in particle number (Fig. 1a) also increased stratus.

The addition of aircraft exhaust slightly decreased the globally- and simulation-averaged in-cloud (for grid-scale clouds) geometric mean number diameter (integrated among all discrete size bins from 0.5 μm to 8-mm diameter) of liquid drops from 17.36 to 17.34 μm, of ice crystals from 42.9 to 41.0 μm, and of graupel particles from 54.5 to 54.2 μm. The reduction in cloud particle size is consistent with the increase in cloud optical depth due to aircraft (+0.51% globally and +0.87% in the Northern Hemisphere) (first indirect effect).

4.3 Effects on global temperatures, arctic temperatures, and sea ice

Aircraft exhaust increased globally-averaged near-surface air temperatures by ~0.01 K and upper tropospheric air temperatures by ~0.03 K, increasing tropospheric stability below cruise altitude and increasing it slightly above cruise altitude (Fig. 1m). The upper tropospheric warming represents ~4% of the up to ~0.8 K observed upper tropospheric global warming that has accumulated based on 1958–2007 radiosonde data.[25] The surface warming represents ~1.3% of the 0.7–0.8 K surface global warming accumulated since 1850.[26]

The modest surface global warming due to aircraft was due to strong Arctic warming offset substantially by midlatitude cooling. Fig. 4 shows the zonal

variation of the near-surface temperature change due to aircraft. It indicates that the strongest warming occurred north of 80 N. Fig. 3b shows that this warming exceeded 1 K over a third of the Arctic above 80 N. Although aircraft slightly cooled the surface at midlatitudes, they warmed the atmosphere at cruise altitude at midlatitudes (Fig. 1m).

Surface warming over the Arctic *versus* surface cooling at midlatitudes was generally due to a combination of (1) the stronger solar effects of aircraft-emitted BC over snow and sea ice than over dark ocean or land surfaces, (2) the fact that aircraft BC has a longer lifetime over the Arctic than at midlatitudes because BC emissions over the Arctic are mostly in the stratosphere,[17] (3) the greater infrared warming than solar cooling due to enhanced cloudiness from aircraft in the Arctic compared with midlatitudes since solar angles are much lower over the Arctic, and (4) the increase in surface pressure (causing air to descend and warm) over the Arctic relative to midlatitudes due to aircraft (Fig. 1o). The increase in Arctic surface pressure may have been due to enhanced poleward motion of air above cruise altitude due to the stronger elevated warming at midlatitudes than at the poles (Fig. 1m), resulting in a stronger pressure gradient between midlatitude and poles. At 11.8 km (200 hPa) and above, warming from 50–70 N exceeded that from 70–90 N. (Fig. 3i, 1m).

Although the global surface warming due to aircraft was small, it was statistically significant in the Arctic region where most warming occurred (Fig. 3c). About 26% of the global surface temperature change was statistically significant to a confidence level (CL) of 95% based on a 2-sided t-test. About 40% was significant to a CL of 85%.

IPCC [2007][9] estimates a 1960–2005 surface air temperature increase north of 65 N of ~1.2 K. Based on computer-generated maps interpolating data,[27] the surface temperature increase north of 65 N from 1880–2008 relative to 1880–1920 was ~2.5 K. In the model, aircraft increased surface air temperatures above the Arctic Circle by 0.1–0.4 K, with an average above the Arctic Circle of ~0.15 K (6% of Arctic warming since 1880). Modeled Arctic ice area simultaneously decreased by 0.03% in the Northern Hemisphere. Sea ice thickness also decreased substantially in the Arctic Circle (Fig. 3j).

Previously, Jacobson *et al.* [2012][18] examined the effect of rerouting aircraft flying over the Arctic to around the Arctic Circle. The study concluded that rerouting would reduce BC and other emissions over the Arctic Circle by ~83% but move the emissions to outside the Arctic Circle and slightly increase fuel use. Moving emissions out of the Circle puts them in regions of greater precipitation, causing a net reduction in particles, which are removed readily by precipitation. The study also found an Arctic cooling due to rerouting of up to 0.3 K in the zonal average, suggesting that higher temperatures over the Arctic were substantially due to local emissions over the Arctic Circle. The present study supports the previous finding that aircraft have a much stronger surface temperature impact over the Arctic region than in the global average. Arctic warming in the present study was up to 0.4 K in the zonal average (Fig. 4).

The results here suggest that, over the Arctic, the relative contribution of aircraft BC (with high BC emissions) to total column BC from all sources is ~10%. Except for some local shipping emissions of BC, aircraft BC represent nearly all BC emissions directly over Arctic sea ice, and such emissions occur in the stratosphere at heights above most. As such, aircraft-emitted BC over the Arctic

has a longer lifetime than does BC emitted from surface sources. BC emissions per unit ground surface area over the Arctic are about 17–33% of the global average aircraft emission density [Table 8 of Wilkerson *et al.*, 2010],[20] suggesting that the emission concentration of BC over the Arctic is significant.

BC emissions from aircraft affect air and surface temperatures in four major ways. First, contrails form on top of emitted aircraft particles, which contain BC coated by lubricating oil, unburned fuel oil, and sulfate. Some BC in the emission plume also coagulates with contrail particles, becoming an appendage or inclusion. When sunlight hits a contrail particle, the light is refracted into it and internally reflected, and some of this light is eventually absorbed by the BC inclusions, increasing cloud absorption. This absorption warms the ice crystal and hence the air around it, causing some melting and sublimation Jacobson [2012].[14] When a contrail particle sublimates, the resulting BC-containing aerosol particle is released to the air and can serve as a nucleus for cirrus or other types of cloud particles. Once incorporated within the cirrus particle, BC can warm the cirrus as well.

Second, aircraft-emitted aerosol particles containing BC that are not incorporated into contrails, but lie between them interstitially, warm the air by direct solar radiative heating (and some infrared heating). Scattering among contrail particles enhances this absorption significantly, as quantified in Jacobson [2012].[14]

Third, BC-containing particles in the air away from clouds reduce the single-scattering albedo of aerosol particles, warming the air due to solar absorption, heating the air, reducing the RH. This warming is enhanced for aged BC particles since such particles become more coated with volatile material as they age, and a coated BC particle warms the air much more than does an uncoated BC particle. This warming is also enhanced over the Arctic compared with midlatitudes due to the higher relative humidity over the Arctic (despite lower column water vapor), which increases the hydration of supercooled liquid water onto soluble material that coats BC, enhancing the coating more. Further, this warming is enhanced over snow, sea ice, and cloud surfaces compared with land, ocean, or cloud-free surfaces since strong reflection allows BC to absorb upward-reflected radiation along with downward radiation. This is one of the main reasons for the enhanced effects of BC over high-albedo surfaces. At night, all contrails and aerosol particles, including BC, increase the downward flux of thermal-IR, warming the surface. Since the Arctic is dark during much of the Northern Hemisphere winter, contrails and particles generally have only a warming effect during the winter.

Fourth, BC-containing particles ultimately deposit to snow and sea ice, primarily by precipitation. The combination of aircraft-emitted BC inclusions within snow and sea ice grains and all feedbacks of aircraft to climate reduced the surface albedo globally here by $\sim$0.1%, warming and enhancing the melting/sublimation of snow and ice, potentially uncovering the lower-albedo ocean or land below.

Despite the fact that aircraft do not fly much over the Antarctic, Fig. 3b and 4 indicates that aircraft emissions globally affected temperatures at the edge of the Antarctic sea ice. Most warming was localized to one particular area (Fig. 3b). This warming was due primarily to the increase in subpolar surface pressure outside the Antarctic polar vortex (Fig. 1o). Temperature and pressure changes in the Northern Hemisphere resulted in enhanced south poleward movement of air. In

the Southern Hemisphere, that air was blocked by the circumpolar jet stream wind system so descended outside the Antarctic. Over the Arctic, the polar vortex is weaker, so poleward air reaches the pole before descending. As the air descended outside the Antarctic, it compresses and warms, melting some snow and ice. In addition, aircraft CO_2 and BC permeated to the Antarctic, where it contributed to some warming there. Since sea ice at its borders is thin, small changes in temperature have a large impact on albedo, since melting uncovers the low albedo ocean below.

4.4 Effects on irradiance

The net (solar+thermal-IR) top-of-the-atmosphere (TOA, at 0.22 hPa or 59.43 km), tropopause (250 hPa or 10.4 km), and surface irradiance changes due to all feedbacks from aircraft were +54, +43, and −86 mW m^{-2}, respectively (Fig. 3h). These are climate response irradiance changes, not radiative forcings. Nevertheless, the 54 mW m^{-2} increase in irradiance at the TOA is not so far from the estimate of 55 mW m^{-2} from Lee *et al.* [2009][10] for the radiative forcing due to aircraft without considering cirrus enhancement and the 78 mW m^{-2} accounting for cirrus enhancement.

4.5 Uncertainties

Uncertainties in the model arise primarily from the coarse horizontal resolution of grid scale treatments, emission data (aircraft, other anthropogenic, and natural), the representation of clouds, the representation of aerosol-cloud interactions, and sub-grid turbulence in aircraft exhaust plumes. Quantifying the possible uncertainty in the mean results presented here due to the uncertainties of these treatments is not trivial. For example, the uncertainty due to resolution alone could not be determined because the computer time for the present simulation was over a year, so increasing the resolution by a factor of 2 in each of the *x*- and *y*- dimensions would result in simulations of over four years, and even this resolution is not sufficient for determining uncertainty. As such, it can only be said that the results presented are those based on the current setup and future work with higher resolution and even more detailed physical treatments is needed to determine the uncertainty of the present results.

5 Summary

This study examined the short term (20-year) effects of contemporary gas and particle exhaust from all commercial flights worldwide on climate and atmospheric composition. Results were obtained assuming constant emissions over this period. The model used, GATOR-GCMOM, treated the emissions and evolution of gas and particle exhaust from each commercial aircraft flight worldwide at the subgrid scale. Aircraft exhaust included CO, CO_2, H_2O, speciated hydrocarbons, NO_x, SO_2, BC, POM, and sulfate. The algorithms used and baseline model results were analyzed against data in Part I of this study, Jacobson *et al.* [2011].[16,18]

Results here indicate that aircraft emissions increased Arctic surface temperatures by ∼0.15 K, global averaged surface temperatures by −0.01 K, and globally-averaged upper tropospheric temperatures by ∼0.03 K, thereby increasing

atmospheric stability below cruise altitude and decreasing it above cruise altitude. Strong Arctic surface warming due to aircraft was largely offset by midlatitude cooling. Cruise altitude temperatures increased substantially both at midlatitudes and over the poles. Overall, surface warming due to aircraft represents ~6% of Arctic surface warming since 1880, ~1.3% of accumulated net global surface warming since 1850, and ~4% of observed upper-tropospheric warming from 1958–2007. Arctic warming due to aircraft slightly decreased sea ice area. Longer simulations should enhance warming due to the further reduction increases in CO_2.

Whereas aircraft emissions decreased cumulus convection by enhancing stability below cruise altitude, they increased stratiform and total cloud fraction on average. Aircraft emissions increased surface and upper tropospheric ozone by ~0.4% and ~2.5%, respectively and surface and upper-tropospheric PAN by ~0.1% and ~5%, respectively. Aircraft emissions increased tropospheric OH, decreasing column CO and CH_4 by ~1.7% and ~0.9%, respectively. Aircraft emissions increased mortality worldwide by ~620 (−240 to 4770) deaths per year, with half due to ozone and the rest to $PM_{2.5}$.

These results suggest that aircraft, particularly their black carbon particle emissions, may have a significant impact on short-term climate, particularly over the Arctic, and chemical composition. The Arctic result is consistent with Jacobson *et al.* [2012], who examined the effect of rerouting aircraft around the Arctic Circle on climate. However, longer-term simulations are needed to account more fully for the effects of carbon dioxide from aircraft on climate and composition. Additional work is needed to improve aircraft emissions inventories, simulate better the contrail-cirrus transition, and reduce the uncertainty due to the coarse resolution of grid-scale processes and of physical treatments in the model.

Acknowledgements

This work was supported by the Partnership for AiR Transportation Noise & Emissions Reduction (PARTNER) and the Federal Aviation Administration (FAA). Any opinions, findings, and conclusions or recommendations expressed in this material are those of the authors and do not necessarily reflect the views of PARTNER or the FAA.

References

1 G. P. Brasseur, R. A. Cox, D. Hauglustaine, I. Isaksen, J. Lelieveld, D. H. Lister, R. Sausen, U. Schumann, A. Wahner and P. Wiesen, European Assessment of the atmospheric effects of aircraft emissions, *Atmos. Environ.*, 1998, **32**, 2329–2418.
2 M. Prather, R. Sausen, A. S. Grossman, J. M. Haywood, D. Rind, and B. H. Subbaraya, Potential climate change from aviation. in *"Aviation and Global Atmosphere", Intergovernmental Panel on Climate Changes*, ed. J. E. Penner, D. H. Lister, D. J. Griggs, D. J. Dokken and M. McFarland, Cambridge University Press, Cambridge, U.K, 1999.
3 P. Minnis, U. Schumann, D. R. Doelling, K. M. Gierens and D. W. Fahey, Global distribution of contrail radiative forcing, *Geophys. Res. Lett.*, 1999, **26**, 1853–1856.
4 G. Myhre and F. Stordal, On the tradeoff of the solar and thermal infrared radiative impact of contrails, *Geophys. Res. Lett.*, 2001, **28**, 3119–3122.
5 M. Ponater, S. Marquart and R. Sausen, Contrails in a comprehensive global climate model: Parameterization and radiative forcing results, *J. Geophys. Res.*, 2002, **107**, 4164, DOI: 10.1029/2001JD000429.

6 S. Marquart, M. Ponater, F. R. Mager and R. Sausen, Future development of contrail cover, optical depth, and radiative forcing: Impacts of increasing air traffic and climate change, *J. Clim.*, 2003, **16**, 2890–2904.
7 P. Minnis, J. K. Ayers, R. Palikonda and D. Phan, Contrails, cirrus trends, and climate, *J. Clim.*, 2004, **17**, 1671–1685.
8 R. Sausen, I. Isaksen, V. Grewe, D. Hauglustaine, D. Lee, G. Myhre, M. Köhler, G. Pitari, U. Schumann, F. Stordal and C. Zerefos, Aviation radiative forcing in 2000: An update on IPCC (1999), *Meteorol. Z.*, 2005, **14**, 555–561.
9 Intergovernmental Panel on Climate Change (IPCC), Fourth Assessment Report, *The Physical Science Basis*, Cambridge University Press, 2007.
10 D. S. Lee, G. Pitari, V. Grewe, K. Gierens, J. E. Penner, A. Petzold, M. J. Prather, U. Schumann, A. Bais, T. Bernsten, D. Iachetti, L. L. Lim and R. Sausen, Transport impacts on atmosphere and climate: Aviation, *Atmos. Environ.*, 2010, **44**, 4678–4734.
11 T. C. Bond, *et al.*, Bounding the role of black carbon in the climate system: A scientific assessment, *J. Geophys. Res.*, 2013, **118**, 5380–5552.
12 M. Ponater, S. Brinkop, R. Sausen and U. Schumann, Simulating the global atmospheric response to aircraft water vapour emissions and contrails. A first approach using a GCM, *Ann. Geophys.*, 1996, **14**, 941–960.
13 D. Rind, P. Lonergan and K. Shah, Modeled impact of cirrus cloud increases along aircraft flight paths, *J. Geophys. Res.*, 2000, **105**, 19927–19940.
14 M. Z. Jacobson, Investigating cloud absorption effects: Global absorption properties of black carbon, tar balls, and soil dust in clouds and aerosols, *J. Geophys. Res.*, 2012, **117**, D06205, DOI: 10.1029/2011JD017218.
15 C. Fromming, M. Ponater, K. Dahlmann, V. Grewe, D. S. Lee and R. Sausen, Aviation-induced radiative forcing and surface temperature change in dependency of the emission altitude, *J. Geophys. Res.*, 2012, **117**, D19104, DOI: 10.1029/2012JD018204.
16 M. Z. Jacobson, J. T. Wilkerson, A. D. Naiman and S. K. Lele, The effects of aircraft on climate and pollution. Part I: Numerical methods for treating the subgrid evolution of discrete size- and composition-resolved contrails from all commercial flights worldwide, *J. Comput. Phys.*, 2011, **230**, 5115–5132, DOI: 10.1016/j.jcp.2011.03.031.
17 D. B. Whitt, J. T. Wilkerson, M. Z. Jacobson, A. D. Naiman and S. K. Lele, Vertical mixing of commercial aviation emissions from cruise altitude to the surface, *J. Geophys. Res.*, 2011, **116**, D14109, DOI: 10.1029/2010JD015532.
18 M. Z. Jacobson, J. T. Wilkerson, S. Balasubramanian, W. W. Cooper, Jr. and N. Mohleji, The effects of rerouting aircraft around the Arctic Circle on Arctic and global climate, *Clim. Change*, 2012, **115**, 709–724, DOI: 10.1007/s10584-012-0462-0.
19 A. D. Naiman, S. K. Lele, J. T. Wilkerson and M. Z. Jacobson, Parameterization of subgrid plume dilution for use in large-scale atmospheric simulations, *Atmos. Chem. Phys.*, 2010, **10**, 2551–2560.
20 J. T. Wilkerson, M. Z. Jacobson, A. Malwitz, S. Balasubramanian, R. Wayson, G. Fleming, A. D. Naiman and S. K. Lele, Analysis of emission data from global commercial aviation: 2004 and 2006, *Atmos. Chem. Phys.*, 2010, **10**, 6391–6408.
21 GFS (Global Forecast System), $1^\circ \times 1^\circ$ reanalysis fields, http://nomads.ncdc.noaa.gov/data/gfs-avn-hi/, 2012, Accessed January 28, 2013.
22 M. Z. Jacobson and D. G. Streets, The influence of future anthropogenic emissions on climate, natural emissions, and air quality, *J. Geophys. Res.*, 2009, **114**, D08118, DOI: 10.1029/2008JD011476.
23 M. O. Köhler, G. Radel, O. Dessens, K. P. Shine, H. L. Rogers, O. Wild and J. A. Pile, Impact of perturbations to nitrogen oxide emissions from global aviation, *J. Geophys. Res.*, 2008, **113**, D11, DOI: 10.1029/2007JD009140.
24 M. Z. Jacobson, The enhancement of local air pollution by urban CO_2 domes, *Environ. Sci. Technol.*, 2010, **44**, 2497–2502, DOI: 10.1021/es903018m.
25 W. J. Randel, *et al.*, An update of observed stratospheric temperature trends, *J. Geophys. Res.*, 2009, **114**, D02107, DOI: 10.1029/2008JD010421.
26 P. Brohan, J. J. Kennedy, I. Harris, S. F. B. Tett and P. D. Jones, Uncertainty estimates in regional and global observed temperature changes: A new data set from 1850, *J. Geophys. Res.*, 2006, **111**, D12106, DOI: 10.1029/2005JD006548.
27 GISS (Goddard Institute for Space Studies), GISS Surface Temperature Analysis, http://data.giss.nasa.gov/gistemp/maps/, 2009, accessed Jan. 19, 2009.

